Brain Research 1826 (2024) 148730

Contents lists available at ScienceDirect

Brain Research

journal homepage: www.elsevier.com/locate/brainres

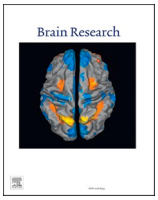

Research paper

The cerebellum monitors errors and entrains executive networks

P. Andre [a,*], N. Cantore [b], L. Lucibello [a], P. Migliaccio [a], B. Rossi [b,c], M.C. Carboncini [b,c,1], A.M. Aloisi [a], D. Manzoni [c], P. Arrighi [b,1]

[a] Department of Medicine, Surgery and Neuroscience, University of Siena, Siena, Italy
[b] Neurorehabilitation Unit, Pisa University Hospital, Pisa, Italy
[c] Department of Translational Research and New Medical and Surgical Technologies, University of Pisa, Pisa, Italy

ARTICLE INFO

Keywords:
Cerebellum
Frontal midline cortex
Visuomotor tracking
Action monitoring
Prediction error
θ rhythm

ABSTRACT

Frontal midline θ (Fmθ) activity occurs in medial prefrontal cortices (mPFC), when expected and actual outcomes conflict. Cerebellar forward models could inform the mPFC about this mismatch.

To verify this hypothesis we correlated the mPFC activation during a visuomotor tracking task (VM) with performance accuracy, in control and cerebellum-lesioned participants. Additionally, purely visual (V), motor (M) and a motor plus visual tasks (V + M) were performed.

An Independent Component, with a mid-frontal topography scalp map and equivalent dipole location in the dorsal anterior cingulate cortex accounted for Fmθ.

In control participants Fmθ power increased during VM, when the error level crossed a threshold, but not during V + M, M and V. This increase scaled with tracking error.

Fmθ power failed to increase during VM in cerebellar participants, even at highest tracking errors.

Thus, in control participants, activation of mPFC is induced when a continuous monitoring effort for online error detection is required. The presence of a threshold error for enhancing Fmθ, suggests the switch from an automatic to an executive tracking control, which recruits the mPFC.

Given that the cerebellum stores forward models, the absence of Fmθ increases during tracking errors in cerebellar participants indicates that cerebellum is necessary for supplying the mPFC with prediction error-related information. This occurs when automatic control falters, and a deliberate correction mechanism needs to be triggered.

Further studies are needed to verify if this alerting function also occurs in the context of the other cognitive and non-cognitive functions in which the cerebellum is involved.

1. Introduction

Motor acts rely on the functional integration of sensory and motor areas of the brain. Sensory information enables us to estimate the state of the peripheral motor plant during motor programming and to assess the effects of a motor command during the execution of a movement. Furthermore, during movement execution, the actual sensory information is confronted to what is predicted based on an internal model (Wolpert et al., 1995). If the predicted and actual signals mismatch, the discrepancy leads to the generation of a sensory prediction error. The brain uses this sensory prediction error in real-time to adjust motor commands, in order to reach the movement goal (Desmurget and Grafton, 2000).

A neuroimaging study that employs an alteration of the visual feedback (using computer-based visual rotation) to induce execution errors, indicates that Frontal cortical regions may be essential for organizing on-the-fly corrections in response to an unexpected trajectory error (Mutha et al., 2011). This finding suggests that Frontal regions may be activated by the sensory prediction error during erroneous motor acts.

Indeed, during motor errors, an increase in θ rhythm indicative of increased activation, is observed in the Frontal midline cortices, namely in the Anterior Cingulate Cortex (ACC; see Arrighi et al., 2016 for ref). Accordingly, in an EEG study conducted during movements with distorted visual feedback, Contreras-Vidal and Kerick (Contreras-Vidal and Kerick, 2004) identified a transient fronto-central θ activity shortly after

* Corresponding author.
E-mail address: paolo.andre@unisi.it (P. Andre).
[1] Deceased.

https://doi.org/10.1016/j.brainres.2023.148730
Received 11 August 2023; Received in revised form 24 November 2023; Accepted 14 December 2023
Available online 19 December 2023

movement onset.

In a task where participants were required to reach targets under prism distortion without visual feedback in the initial part of the hand trajectory, Frontal midline theta (Fmθ) rhythm increased only when motor errors induced by the visual shifts exceeded a certain threshold (Arrighi et al., 2016). Above this threshold, the increase in Fmθ scaled with the degree of motor error, exhibiting an approximate delay of 200 ms after the onset of visual feedback. These findings strongly suggest that the increase in Fmθ is dependent on visuomotor prediction errors.

This hypothesis was proved by Savoie et al. (Savoie et al., 2018) who documented that visuomotor prediction errors rather than reward errors lead to an increased θ power (and to a Feedback Related Negativity-like potential) over mid-frontal scalp sites.

Interestingly, the midline frontal cortices (ACC) are activated in tasks of focused attention (Ishii et al., 1999) and activation of these structures elicit an increase of Fmθ (Pizzagalli et al., 2003). Both ACC and Fmθ seem particularly involved in error processing (Falkenstein et al., 1991; Carter et al., 1998; Kiehl et al., 2000) and detecting conflict between information and/or responses. This hypothesis has being proposed since Fmθ and ACC activation occur when the subject is exposed to tasks that require overriding dominant response tendencies (such as in the Stroop, flanker, Simon task, and go/no-go paradigm) or selecting among equally permissible responses (see Botvinick, 2007 for ref.). Additionally, the ACC is implicated in tasks that involve dividing attention between competing tasks (Corbetta et al., 1991).

Numerous models have been proposed to explain the activation of frontal midline structures and the emergence of θ activity following a task-related error (see Arrighi et al., 2016 for ref.). In light of the cerebellum's implication in prediction error (Popa and Ebner, 2019; Tanaka et al., 2019; Kakei et al., 2019; Tanaka et al., 2020; Gatti et al., 2021) we speculated that it may be an important node within the network responsible for activating the Frontal midline executive regions when the predicted error cannot be rectified by implicit/automatic systems, but instead requires explicit corrective mechanisms (Andre and Arrighi, 2003).

A substantial body of behavioral, neurophysiologic, imaging and modeling studies (Flament et al.,1996; Imamizu et al., 2000; Diedrichsen et al., 2005; Grafton et al., 2008; Schlerf et al., 2012; Streng et al., 2018a; Streng et al., 2018b; Popa and Ebner, 2019) supports the original proposal that the cerebellum may acquire and store forward models of the body for predictive movement control (Miall et al., 1993; Diedrichsen et al., 2007; Miall et al., 2007; Popa et al., 2013; Popa and Ebner, 2019).

To the best of our knowledge, there is currently no evidence indicating that the prediction error generated by the forward model in the cerebellum (Wolpert et al., 1998) can simultaneously engage the frontal executive network. Such engagement may occur when the movement is significantly altered, necessitating the involvement of the executive network to achieve the intended goal.

The cerebellum may thus become an essential component of an alert system when automatic processing fails.

Supporting evidence for this hypothesis is the fact that prefrontal regions, including the medial prefrontal cortex, are indeed sensitive to prediction errors. In fact, prediction errors generate frontocentral negative potentials, with sources that include the medial prefrontal cortex (Torrecillos et al., 2014).

Various pathways, both direct or indirect (including transcortical) pathways, may convey the error signal generated by the cerebellum to the ACC. Notably, there are reciprocal connections among cerebellar, parietal and prefrontal cortices (Ramnani, 2006; Strick et al., 2009). In humans, neuroimaging studies show that several important networks including Fm structures are related to focal areas within the posterior lobe of the cerebellum (Kipping et al., 2013; Schmahmann, 2019; Habas, 2021).

In animals, anatomical studies utilizing virus or fluorescent anterograde/retrograde tracers have identified projections from the cerebellum to prefrontal and posterior parietal cortical areas which participate in executive functions, performance monitoring, and movement control (Giannetti and Molinari, 2002; Dum and Strick, 2003; Strick et al., 2009). The cingulate cortex may also receive a cerebellar input via the thalamic nuclei centralis lateralis (CL) and medial dorsal nucleus (MDn) (Schmahmann, 1996).

Finally, connections from the anterior cingulate cortex to the cerebellum have also been described (Brodal, 1978; Vilensky and Hoesen, 1981; Glickstein et al., 1985; Ramnani, 2012).

As a functional evidence, at least one electrophysiological study in humans, utilizing single-pulse transcranial magnetic stimulation (TMS), has shown that the cerebellum can evoke θ activity within the frontal cortex (Schutter and van Honk, 2006).

The present study was designed to test the aforementioned hypothesis, namely that in addition to its well-known processing capabilities, the cerebellum also acts as an alerting system under unexpected results. Through this function, the cerebellum would play an active role in shifting between automatic and attentional processing. Specifically, our aim was to address the question of whether the cerebellum serves as a hub for activating frontal midline cortices during error processing.

To achieve this goal we developed a visuomotor tracking task and investigated the correlation between changes in Fmθ and tracking errors in both healthy individuals and in subjects whose cerebellum was partially knocked-out by a pathological event.

We chose a visuomotor tracking task, which requires cooperation between visual and motor areas of the brain (Classen et al., 1998), for several reasons. This task relies on the cerebellum, as it is impaired by cerebellar lesions (Liu et al., 1999). Visuomotor tracking forces the subjects to continuously monitor their performance and necessitates a forward model to compare the expected outcomes of their action with the actual observed results (Miall et al., 1993). It is supposed that this model is stored in the cerebellum (Miall et al., 1993) which has the capacity to process retinal and proprioceptive signals, receive an efferent copy of the motor command and has an output to the cerebral cortex (Ito, 2005). The cerebellar activation observed during a tracking movement is consistent with the updating of internal models (Imamizu et al., 2000).

As a first step, in the present investigation, we tested in control participants whether the tracking task was capable of eliciting Fmθ in comparison to other tasks (Classen et al., 1998), which impose less burden on the on-line control of the performance. Secondly, we examined whether the Fmθ observed during the tracking task scaled with the degree of motor error. Finally we compared the results obtained in control participant to those obtained in participants with a cerebellar injury.

2. Materials and methods

2.1. Participants

Eight participants with clinical and radiological evidence of a mainly unilateral lesion of the cerebellum (4 females, mean age 42 ± 16 y) and 11 control participants (6 females, mean age 27 ± 7 y, 2 left-handed) devoid of neurological deficits were recruited in the study. Both cerebellar participants and control participants underwent a comprehensive neurological examination.

As shown in Table 1, all cerebellar participants were characterized based on 1) impaired cerebellar function and 2) anatomical location of the cerebellar lesion (identified through CT and/or MRI imaging). Among the cerebellar participants, the cerebellar lesion was of vascular in origin for 6 participants (haemorrhagic n = 3, ischemic n = 3) while it was neoplastic in the remaining 2 participants. For most of the cerebellar participants the lesion and the resultant motor deficits were confined to one side (see Table 1). In the two participants with bilateral lesions, motor impairment was not equivalent on both sides, allowing for a clear distinction between a less impaired and a more impaired side. The study

Table 1
Characteristics of cerebellar participants. The table gives the patient identification number, age, sex, and clinical data, including the gravity score of the main symptoms. -: not present. +: mild; ++: moderate, +++: severe. Upper and lower limb ataxia scores refer to the "more affected side" reported in the sixth column from the left.

Patient	Age (years)	Sex	Time from lesion exordium	Location of the cerebellar lesion	Affected-more affected side	Aetiology	Postural ataxia	Upper limb ataxia	Lower limb ataxia	Dysarthria	Oculomotor deficits
1	52	M	1 month	Right Hemivermis, Right Hemisphere, Right inferior and medial cerebellar peduncles	Right	Ischemic	+++	++	+	++	+
2	35	F	18 months	Left Hemivermis, Left Hemisphere	Left	Haemorrhagic	_	+++	+++	++	++
3	24	M	18 years	Left Hemivermis, Left Hemisphere	Left	Neoplastic	++	+	+	_	_
4	60	F	1 year	Right Hemivermis, Right Hemisphere	Right	Ischemic	++	+	+	_	_
5	38	M	1 month	Left Hemivermis, Left Hemisphere	Left	Ischemic	++	++	++	_	+
6	26	F	1 year	Left Hemivermis, Right Hemivermis	Left	Neoplastic	+++	++	++	+	+
7	68	F	3 years	Right Hemivermis, Right Hemisphere	Right	Haemorrhagic	+	+	+	+	+
8	30	M	2 months	Left Hemivermis, Right Hemivermis	Left	Haemorrhagic	+++	++	++	+	+

received approval by the Ethical Committee of the Siena University (endorsement 62/2022) and was conducted in accordance with the "World Medical Association Declaration of Helsinki". All participants provided informed consent.

2.2. Experimental protocol

During an experimental session, both cerebellar and control participants were engaged in the following sequences of tasks, each lasting 120 s, while comfortably seated in a chair (Fig. 1A):

1) pure visual (V),
2) pure motor (M),
3) visual plus motor (V + M) and
4) visuomotor (VM).

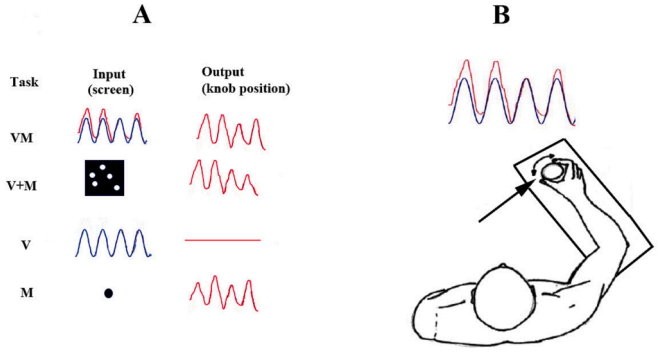

Fig. 1. *Experimental tasks and setup.* A. The different tasks performed by the participant are indicated on the left. VM: visuomotor. V + M: visual plus motor. V: visual. M: motor. The visual display presented to the participant during the different tasks is shown in the column "Input". The output of knob (see B), representing the participant tracking performance is illustrate in the column "Output". Please note that the participant receives visual feedback about his performance only during the VM task. B. The participant is seated on an armchair in front of an oscilloscope screen, performing the task VM indicated in B. By rotating the knob (arrow) with the hand, he controls a moving trace on the screen (in red), attempting to superimpose it on a blue target moving sinusoidally along the vertical axis while sweeping from left to right at constant speed.

Before starting each task participants were required to relax and abstain from movements for a (rest) period of the same duration as that of the task. In a subgroup of compliant participants (see *2.9*), the rest period and VM task were repeated up to six times following the completion of the regular sequence 1–4. These additional recordings allowed us to gather sufficient data to determine tracking accuracy (see *3.1*) and its relation with the EEG activity during VM (*see 3.4*).

Both groups of control and cerebellar participants, underwent two experimental sessions scheduled between 9 a.m. and 12 a.m. on non-consecutive days. Control participants performed the tasks using their dominant hand during the first day and their contralateral hand during the second day. Cerebellar participants utilized their more impaired hand on the first day and their contralateral one (less or non-impaired hand) on the second day.

2.3. Tasks

The investigation took place in a quiet room with subdued lighting. The experimental setting is illustrated in Fig. 1. Throughout the rest periods, participants focused their gaze on a stationary (black) dot (2 cm in diameter), printed on a white board that covered the screen of a dual colour trace (red and blue) oscilloscope. The board was positioned at eyes level, 1 m in front of the participants. During the rest period the oscilloscope traces were off and the participants were required to refrain from any body movement.

During the visual task (V) the white board was removed, and participants were instructed to observe the oscilloscope blue trace which moved sinusoidally along the vertical axis at the frequency of 0.25 cycles/sec, with a peak-to-peak amplitude of 4 cm (equivalent to a visual angle of 4° (Fig. 1A, V). As the blue trace underwent its sinusoidal motion along the Y axis, it continuously shifted from left to right along the X axis at the constant sweep speed of 0.625 cm/sec, so that the oscilloscope screen displayed four compete sinusoids (Fig. 1A). The motion of the blue trace was controlled by a signal generator (Wavetek 175, Waveteck San Diego Inc., San Diego, California, USA). Throughout the task the participants were required to refrain from any body movements.

During the integrative visuomotor tracking task (VM) participants operated the oscilloscope's red trace, attempting to superimpose it on the sinusoidally moving blue trace (target signal) (Fig. 1A, VM; Fig. 1B). To control the red trace participants, utilized a knob (3 cm in diameter)

of a potentiometer positioned on the chair's armrest which was turned, between the forefinger and thumb (Fig. 1B). The potentiometer's output at midpoint turning was calibrated so to align with the zero level of blue trace.

During the motor (M) task (Fig. 1A, M), participants were required to replicate from memory the sinusoidal motion of the blue trace, which they had previously observed, by piloting the potentiometer. Participants were instructed to focus on the black dot positioned at the centre of the white board that covered the oscilloscope screen. This setup ensured that visual feedback regarding performance was unavailable.

Finally, in the visual plus motor task (V + M) participants were required to replicate the same motor output as in VM and M while gazing to a matrix of LEDs, lighted in a random pattern which was positioned on a black cover that obscured the oscilloscope screen (Fig. 1A, V + M). This stimulus did not provide any feedback on their performance.

Each task and its relative rest period lasted for 120 sec with the VM condition being repeated up to 6 times based on the participant's compliance.

2.4. EEG and polygraphic recordings

EEG activity was continuously acquired from 19 channels by using passive silver-plated cup electrodes filled with a conductive paste (Ten20, Weaver, Colorado, USA). The electrodes were embedded in an elastic head cap accordingly with the standards of the 10–20 International System of electrode placement. Recordings were referenced online to a pole formed by short-circuiting the two mastoid electrodes. To enhance the detection of ocular movements or blinks-related artifacts, electrooculographic activity (EOG) was recorded using a pair of surface silver-plated cup electrodes placed at the top of the right outer canthus and at the bottom of the left outer canthus. Bipolar electromyographic (EMG) activity was recorded from the first dorsal interosseus muscle of the moving hand to confirm the execution of the tasks including a motor component, and to monitor undesired muscle activity during rest periods. To facilitate the removal of artifacts associated with electrical heart activity, the ECG signal was recorded bipolarly using two surface electrode placed on the right shoulder and on the position of the V6 chest electrode. EEG, EMG, ECG and EOG activities were band pass filtered (2.5.–50.0 Hz), sampled at 256 Hz and digitized at 12 bits (HandyEEG, Micromed, Verona, Italy). Throughout the entire experimental session, the input impedance of EEG electrodes was kept below 5 kΩ.

The signals from the target (blue) and participant-driven (red) traces (reflecting the tracking performance of the participants) were both fed to an analog-to-digital converter (256 Hz, 12 bit), stored on a separate computer and utilized offline to calculate the positional error during tracking (Fig. 2B).

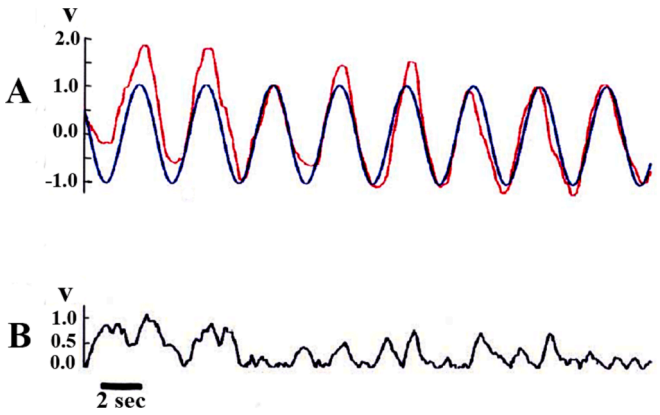

Fig. 2. *Visuomotor tracking and tracking error.* A. Blue and red traces represents the target position and the simultaneous tracking signal generated by the participant, respectively. B. Time course of the tracking error, defined as the absolute difference between the target and the tracking signal.

This value corresponded to the absolute difference between target position and participant-driven trace. A TTL pulse, generated at the beginning of each rest/task period was directed to one channel of the EEG recorder. It was also used to trigger the analog-to-digital converter, thereby synchronizing acquisition of EEG, target and participant-driven trace.

To study the relation between EEG changes and tracking error all the EEG traces, the target trace and the participant-drive trace were segmented in 2-sec epochs.

2.5. Signal processing

The polygraphic data were analysed offline using the EEGLAB toolbox (Swartz Center for Computational Neuroscience, La Jolla, CA; https://www.sccn.ucsd.edu/eeglab; see Arrighi et al., 2016). EEG data were digitally filtered with a band-pass of 2.5–40 Hz and re-referenced to a common average reference. Initially, the data were segmented into epochs of 2 sec. The individual traces were visually inspected to identify and reject artefacts caused by gross participant movements or other sporadically occurring sources (for example: cable movements). This procedure prevented any potential impact of "non-stereotyped" noise on the independent components analysis (ICA). The same segmentation into 2-sec epochs was also applied to the synchronized tracking error signal to maintain one-to-one correspondence with the EEG-derived signal.

2.6. ICA decomposition

The polygraphic (EEG, EOG, EMG and ECG) signals underwent Independent Component Analysis (ICA), which allows the blind separation of input data into temporally independent and spatially segregated components. When applied to EEG signals this technique enables the separation of the various EEG signal sources commonly mixed at the individual electrode level. The purpose of this approach was two-fold: 1) to detect and subsequently remove the EEG artifacts resulting from factors such as muscle activity, eye movements and blinking; and 2) identify the signal source accounting for the frontal midline θ.

For each subject the 22 polygraphic signals (19 EEG, 1 EOG,1 EMG, 1 ECG) relative to a minimum of 8 EEG periods (4 periods of rest and 4 periods of task; total time: 120 s x 8) were initially concatenated. This concatenation resulted in a matrix with dimension of at least of 22 x 245760 (120 s x 256 sampled points/sec x 8 periods). This matrix underwent decomposition using the FastICA algorithm implemented by the FastICA package (Hyvärinen and Oja, 2000, available from https://research.ics.aalto.fi/ica/fastica/code/dlcode.shtml) for decomposition in Independent Components (ICs). During the decomposition process, the settings for "decorrelation approach" and "nonlinearity" were "symmetric" and "tanh", respectively. This procedure resulted in an extraction of 22 ICs, each corresponding to a time series containing a minimum of 245760 points.

An estimate of the reliability of the ICs was achieved by running the ICA algorithm many times (n = 20) with random initial conditions and visualizing their clustering in the signal space by means of the Icasso software package for MATLAB (Himberg et al., 2003, 2004; available from https://www.cis.hut.fi/projects/ica/icasso). When an IC has good statistical reproducibility, its repeated evaluations yields similar outcomes, well segregated from those of other ICs as shown by cluster analysis. The outcomes of these procedures can be visualised in a two-dimensional similarity graph (Himberg et al., 2003, 2004). In the present study, the algorithm was configured to generate 22 clusters, corresponding to the dimension of EEG data. To identify the most compact and isolated clusters that represent the statistically reliable components, a quality index (Iq) was employed (Himberg et al., 2003, 2004). For an ideal cluster, Iq equals 1 with decreasing values indicating less compact

and isolated clusters.

In addition, by combining information from several runs, the algorithm returns a set of 22 components that is considered more accurate compared to any set provided by a single run (Himberg et al., 2003, 2004).

2.7. Dipole source modelling

The scalp maps of the ICA components resembled the projection of a single equivalent dipole, reflecting the synchronous activity of a relatively small portion of cortical territory (Delorme et al., 2012); the location of this dipole within the brain was determined on the basis of the topographic projection of its activity on the scalp. In quantitative terms, this process identify a single equivalent dipole for a given IC that accounts for its topographic projection with minimal residual variance. Hence, we computed an equivalent current dipole model for each brain IC using a standard four-shell spherical head model (radii in mm: 71, 72, 79, 85; conductivity in S/m: 0.33, 1, 0.0042, 0.33). This process was carried out utilizing the DIPFIT toolbox within the EEGLAB software package (accessible from https://www.seen.ucsd.edu/eeglab/dipfit.html). The goodness of fit for modelling each IC with a single dipole was quantified; components were discarded if their best-fitting dipoles were located outside the model brain volume or if they exhibited more than 20 % residual variance.

2.8. Analysis of task related spectral power

These analyses were not conducted on the raw EEG signals but rather on the ICs obtained from ICASSO. For all participants, a minimum of 120 sec of rest and 120 sec of activity were obtained for tasks V, M, V + M and VM: these data served to compare differences in EEG reactivity across the different tasks. The power spectral density (PSD) was measured using the Welch's averaged, modified periodogram method as implemented with the 'pWelch' function of Matlab. According to the algorithm each signal (rest or task) lasting 120 sec was segmented into 119 epochs of 2 sec (512 data points) with 50 % overlap. Each segment was windowed with a Hamming window to minimize spectral leakage. The Direct Fourier transform (DFT) length was set to 1024 points, so that the frequency resolution of the power spectrum corresponded to a bin of 0.25 Hz. Following Classen et al. (Classen et al. 1998), task-related power (TRPow) was expressed as the percentage change of spectral power during tasks compared to rest (TRPow = [(Powtask-Powrest) x 100/Powrest]) in order to reduce the effect of inter-subject variability.

Task-related power changes in ICs components were studied within the α band (α band desinchronization, Neuper et al., 2006), where they indicate cortical recruitment, as well as in the θ band, which reflect the participant's performance (Arrighi et al., 2016).

The alpha band desinchronization was calculated within the frequency range 8–14 Hz. The spectra of individual participants were averaged (point to point), for both the rest and task conditions and the corresponding 95 % confidence interval was calculated.

Spectral power in the θ band was also calculated with frequency ranges tailored for each participant. For each participant, theta band limits were adjusted using the Individual α Frequency (IAF) at rest as an anchor point. IAF represent the frequency corresponding to the highest power density at rest within the range of 6 to 14 Hz. IAF was determined from a reconstructed EEG pruned by the ICs corresponding to artefacts. The IAF value was obtained by averaging its value across electrodes. Then, θ band power was computed for individual ICs as the mean power obtained within the frequency band from IAF minus 6 Hz to IAF minus 4 Hz (Klimesch, 1999).

2.9. Quantification of participant performance and EEG correlates during the visuomotor task

Tracking error estimate were obtainable from all 11 control and from 5 out of 8 cerebellar participants performing the VM task up to 6 times (12 min). Among the 11 control participants, tracking error estimates were taken for the dominant hand in all the participants and for the non-dominant hand in seven of them. Among the 5 cerebellar participants tracking error estimates were taken in all the participants for the more affected hand and in 4 of them for the less affected hand.

The tracking error during VM was expressed as the absolute difference between the target and the participant-driven traces. It was calculated for each of the 2-sec segments in which the task was split and normalized with respect to the average amplitude of the rectified target trace (blue trace in Fig. 2) over the corresponding time intervals. This process yielded an error score where zero represented perfect tracking and a value near or greater than 1 a highly degraded performance (Fig. 2B).

For studying the relation between Fmθ and tracking error, EEG epochs (2 sec) were paired with their corresponding tracking error value. In this analysis a given participant contributed 150 epochs (300 sec) which were sorted according to the tracking error. Such amount of EEG data was obtained in a reasonable number of subjects limitedly to the dominant hand of control participants (n = 11) and to the more affected hand of cerebellar participants (n = 5). The 150 epochs were concatenated and partitioned in three quantiles (low, high, medium) resulting in three datasets of 50 epochs associated to low, medium and high error values. EEG data relative to the epochs of each quantile were concatenated to yields 3 periods of 100 sec duration. In this way we obtained EEG segments relative to periods of low, medium, and high tracking error.

2.10. Statistics

Spectral power values were Log transformed for obtaining a normal distribution of the data. As an initial step, the statistical significance of spectral changes in θ power was evaluated using paired t-tests between task and rest for each condition (VM, V, M, V + M). This analysis was performed for both control and cerebellar participants. The statistical power associated with these comparisons was evaluated by the G*power program (https://www.psychologie.hhu.de/arbeitsgruppen/allgemeine-psychologie-und-arbeitspsychologie/gpower).

Then, differences in Fmθ changes among tasks and hands were separately assessed in both control and cerebellar participants using a 4 Task (V, M, V + M, VM) x 2 Hand repeated measures ANOVA.

To evaluate differences between control and cerebellar participants in the Fmθ changes observed for the VM task, a univariate ANOVA (Control, Cerebellar) was utilized. The effect of introducing age as a covariate in the model was examined.

The relationship between Fmθ changes and the tracking error was separately assessed in both control and cerebellar participants by comparing the Fmθ changes across the three tracking error quantiles (see *2.9*). For this purpose, a 3 Error Level (High, Medium and Low) repeated measures ANOVA was conducted.

A 3 Error Level repeated measure ANOVA with Group as a between subject factor was run to compare control and cerebellar participants relatively to different classes of tracking error.

Finally, to assess Group differences in the scaling between Fmθ changes and tracking error, the difference in Fmθ change between High and Low error quantiles was evaluated for each subject and divided by the corresponding difference in tracking error. This parameter, which represent the change in Fmθ per unit error, was submitted to a univariate (Control, Cerebellar) ANOVA.

The threshold for significance was set at $p < 0.05$. P values relative to multiple paired *t*-test performed between the rest and task conditions as well as post-hoc comparisons in the ANOVA underwent Bonferroni's correction for multiple comparisons.

3. Results

3.1. Accuracy of the VM tracking task in control and cerebellar participants

An example of VM tracking is illustrated in Fig. 2A for a representative case. The relative accuracy is shown in Fig. 2B displaying the absolute difference between target and tracking trace. The grand average positional error calculated across all control participants throughout the entire task duration was 0.37 ± 0.07, SD (n = 11) and 0.36 ± 0.09, SD (n = 7) for the dominant and non-dominant hand, respectively. These results indicate a fair control of the visuomotor performance with no significant differences between the two hands (*t*-test, t = 0.265, p = 0.7940, power = 0.082).

The performance of cerebellar participants with their more affected hand (ipsilateral to the lesion) and less affected hand (contralateral to the lesion) corresponded to 0.65 ± 0.15 (SD, n = 5) and 0.44 ± 0.14 (SD, n = 4), respectively. The difference between these values was not statistically significant (*t*-test, t = 2.15, p = 0.069, power = 0.71). The tracking error of the more affected hand was significantly different from that of both dominant (*t*-test, t = -5.21, $p < 0.0005$, power = 0.99) and non-dominant hand of control participants (*t*-test, t = 4.21, p = 0.0018, power = 0.98). No significant difference could be observed in the tracking performance when the less affected hand of cerebellar participants was compared to both hands of control participants (dominant hand: t = 1.32, p = 0.2096, power = 0.31; non- dominant hand: t = 1.15, p = 0.2798, power = 0.28).

3.2. ICA analysis and identification of selected components

EEG data were analysed by ICA to unveil the dynamics of the cortical source of the EEG frontal θ rhythm. This analysis generated 22 components which were segregated into clusters and characterized by Iq values > 0.90, (see Fig. 3 for a single participant).

Out of the 22 components, only 7 showed comparable power spectrum at rest and had similar scalp map topographical distribution and dipole localization across all control and cerebellar participants. The reliability of these 7 components was established through the correspondence between their topography and their differential reactivity to the performed tasks (see 3.2.1).

The clusters corresponding to the selected components are marked by arrows in Fig. 3 for a representative participant. They have been named as IC1-IC7, following to the order of their description. The scalp map of each component (Fig. 4), peaked around the location of a specific electrode, whose acronym is indicated (between parenthesis) in Fig. 3. All these ICs formed compact and isolated clusters with very high Iq. The average Iq values across participants (n = 19) ranged from 0.92 ± 0.08 (IC5) to 0.98 ± 0.03 (IC6), without differences between control and cerebellar participants (Fig. 3).

3.2.1. Topological aspects of the selected components

Scalp maps inspection revealed a single onion-like field centred at a specific scalp location which suggested that the activity might be generated by a single dipolar brain source. Indeed, a single equivalent current dipole model fitted the scalp map distribution with a residual variance of less than 15 %. This held true for each of the 7 ICs, across both cerebellar and control participants.

Fig. 4 shows scalp maps and power spectra at rest for the 7 selected ICs obtained from a representative participant. The average ICs Talairach coordinates of dipoles (evaluated across participants) closely corresponded in control and cerebellar participants and single ICs sources

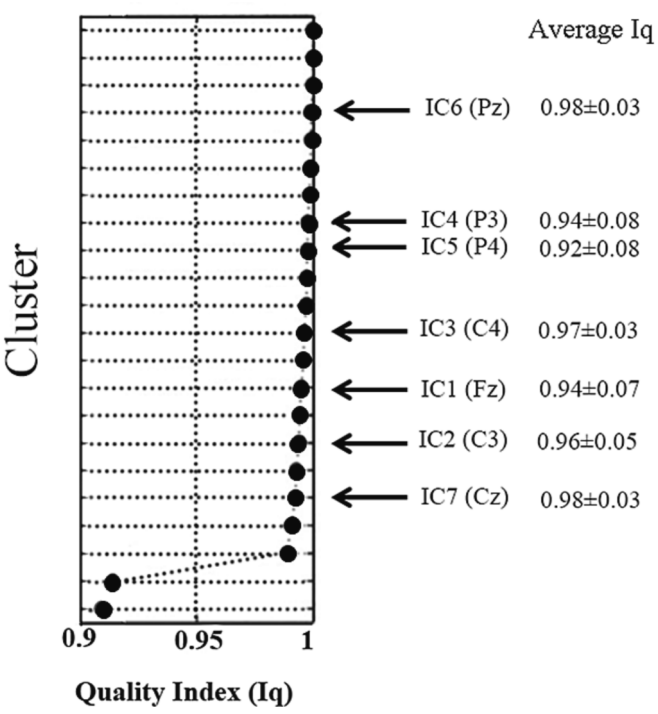

Fig. 3. *Statistical validation of ICAs by ICASSO.* The 22 IC clusters corresponding to the ICASSO's output obtained from a representative participant (dots) have been ranked along the ordinate according to their quality index (Iq) values displayed in abscissas. The cluster at the top is the most compact and isolated. The IC indicated by the arrows have been selected for further analysis as indicated in the text. They have been numbered according to the order of their description in the Result section. The sites were the scalp map of these selected ICs focused is indicated in parenthesis. Mean ± SD values on the right represent the average values obtained for each IC across the whole population of control participants and cerebellar patients (n = 19).

overlapped substantially in brain space between the two populations. Fig. 5A and 5B illustrate this overlap for IC1 and IC6, respectively.

The power spectrum of IC1 included a dominant θ peak and its scalp map projection was centred around the Fz electrode (Fig. 4), being therefore attributable to the Frontal midline θ activity (Fmθ, see Onton et al., 2005). The dipole location of IC1 is illustrated in Fig. 5A, for each control and cerebellar participant. The source of this activity was identified within the anterior cingulate cortex, specifically BA 24/32, at average Tailarach (x, y, z) coordinates of 0.47, 35, 23 for control participants and 1.16, 30.6, 22.5 for cerebellar participants.

IC2 and IC3 components showed a typical sensorimotor μ spectral profile, characterized by α e β components and by a scalp map centered on the central derivations C3 and C4 over the sensory-motor strip (see Fig. 4). Mean equivalent dipoles locations of IC2 (left) and IC3 (right) were in the precentral/postcentral gyrus (BA 4 and BA 3,1,2). As would be expected for activity related to the motor regions, the α rhythm desynchronised during the motor and visuomotor tasks (M, VM and V + M) but not in the purely visual task (V). This phenomenon took place in each control and cerebellar participant: Fig. 6A shows the average α power of IC2 and IC3 relative to all cerebellar and control participants in the different task conditions.

IC4 and IC5 showed a prominent component in the α band at rest and their scalp maps focused over the left and right parietal regions corresponding to P3 and P4 electrode locations (see Fig. 4). Single dipoles of IC4 and IC5 were located within the associative left (BA 39) and right posterior parietal cortex (BA 40). In all participants, as expected for a signal source located into the associative parietal cortex, spectral power in the α band of IC4 and IC5 was suppressed during the integrative VM task, but not during M, V + M and V (Fig. 6B), consistently with the well-

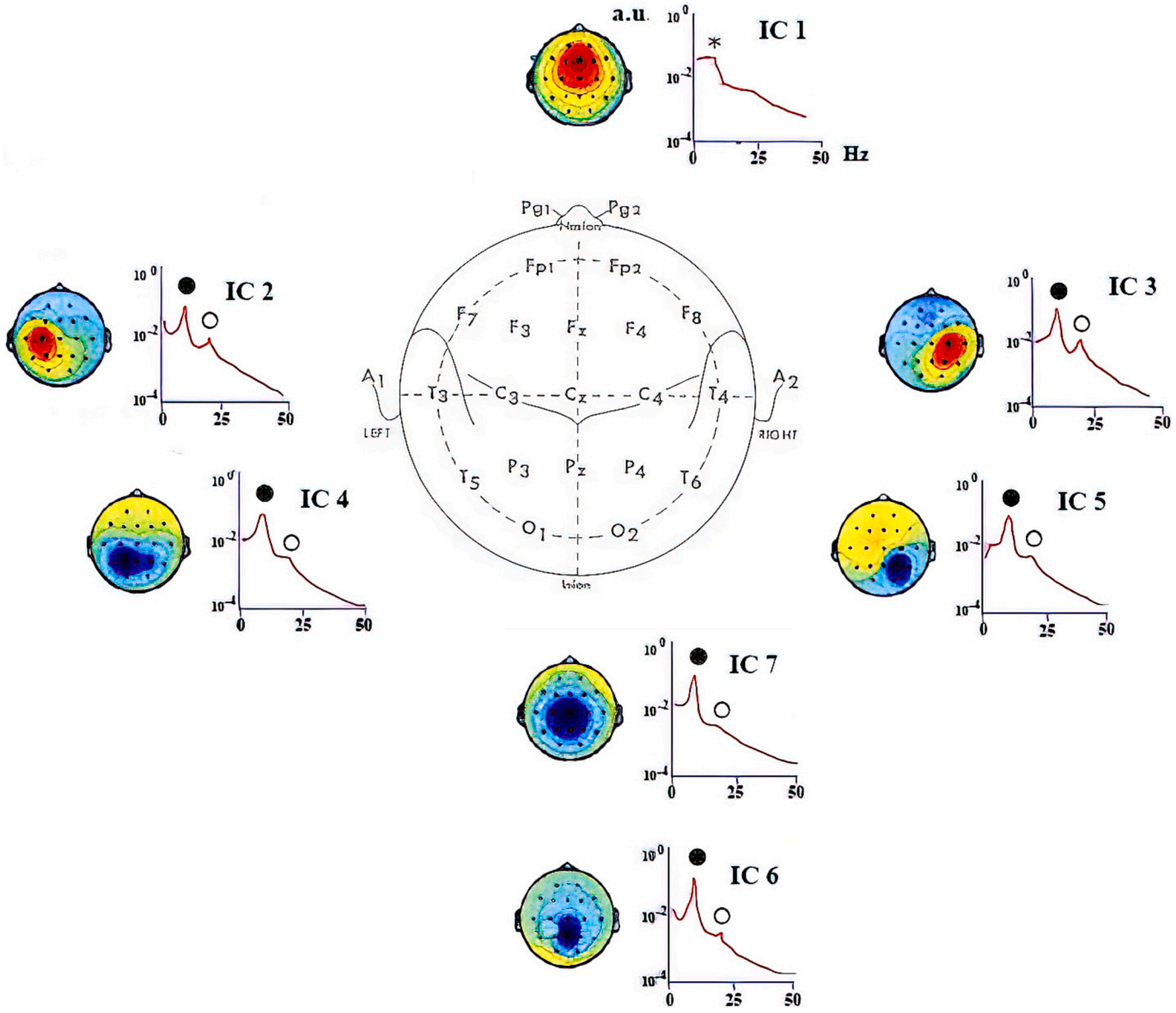

Fig. 4. *Scalp maps and power spectrum at rest of the IC selected for the analysis.* Scalp maps and power spectra of each individual IC, obtained from a representative control participant, have been displayed side to side. Asterisks indicate the θ activity which dominates in the power spectrum of IC1, while black dots and circles indicates the α and β activities, respectively.

known role of parietal cortex in visuomotor behaviour.

IC 6 showed an onion like scalp map overlying the Pz electrode: its dipole location fell within the medial parietal lobe, namely in the precuneus (BA 7). Distribution of IC 6 sources in control and cerebellar participants is shown in Fig. 5B, lower panel. In IC 6 the α rhythm was largely predominant at rest and was suppressed, for both cerebellar participants and controls, in the integrative VM task and, to a minor extent, in the pure visual task, as it could be expected for a parietal region having "a central role….in a wide spectrum of highly integrated tasks including visuospatial imagery" (Cavanna and Trimble, 2006; Cavanna, 2007).

Finally, IC 7 presented a spectral activity predominantly in the low medium frequency ranges (upper θ and α); its equivalent dipole location was consistent with a source in superior medial frontal gyrus near the cingulate motor area (BA 6).

In conclusion, by considering together the spectra at rest, the pattern of spectral reactivity across the different tasks and the topographical localization, it becomes apparent that the ICA identifies components that could be ascribed to the activity of brain areas supporting specific functions. Thus, the IC1 source seems particularly suitable for investigating the changes in θ activity linked to error signal processing within the medial prefrontal cortex.

3.3. *Fmθ activity increases during integrative visuomotor tracking behaviour in control but not in cerebellar participants*

During the VM task, in control participants, θ power of IC1, which expresses the activity of frontal midline cortices, significantly increased (see Table 2A) with respect to the resting state. This increase was observed irrespective of whether participants performed the task with their dominant (Fig. 7:left graph, black dots) or non-dominant hand (Fig. 7:left graph, black squares), as evaluated by paired *t* test.

The increase in Fmθ activity in % of the rest condition value corresponded to + 29 ± 19.9, SD, % (n = 11) for the dominant and to + 23.1 ± 12.9, SD, % (n = 8) for the non-dominant hand (Fig. 7:left plot and Table 2A). This increase was not observed during the other motor tasks (M and V + M), which do not necessitate stringent evaluation of the performance, nor during the visual (V) task (see Fig. 7:left plot and

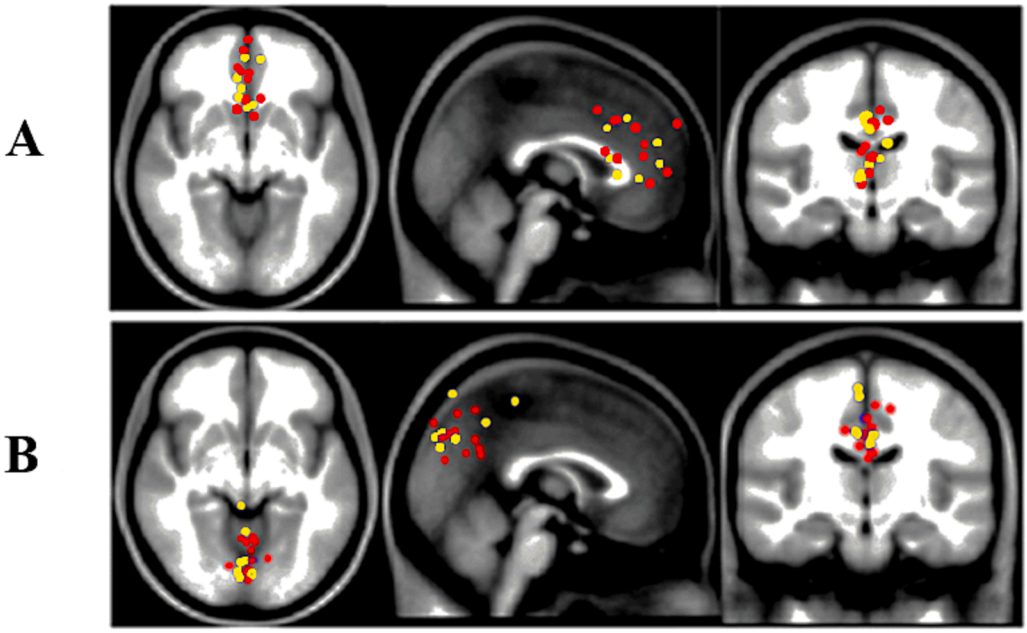

Fig. 5. *Localization of the dipoles associated to IC1 and IC6.* Localization of the dipole associated to IC1 (A) and to IC6 (B) scalp maps analysed have been reported for all the participants. Both in A and in B yellow and red dots represent cerebellar and control participants, respectively. Dipoles have been localised within a 85 mm ray spherical, 4 shell head model (skull, epidural space, meninges, brain), co-registered with the Montreal Neurological Institute average MRI image.

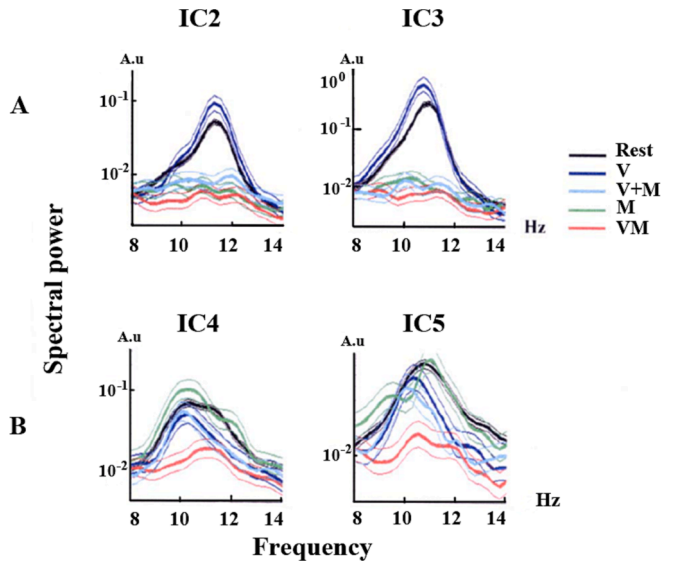

Fig. 6. *Task-related α desynchronization affecting IC2-IC5.* Grand-average α band Power spectrum values (arbitrary units) observed during different tasks and at rest for IC2, IC3, IC4 and IC5. Control and cerebellar participants were pooled together. Task/rest conditions are indicated by different colours. Thinner lines represent 5 % confidence intervals of the mean. Note that IC2 and IC3 (related to central activities) decrease the α band power in all the task including a motor component, i.e. VM, M and V + M, while IC5 and IC5 (related to parietal activities) show α desynchronization only during the integrative visuomotor (VM) task.

Table 2A).

It must be pointed out that when the changes in Fmθ were analysed with a 2 Hand (dominant, non-dominant) x 4 Task (VM, M, V + M, V) ANOVA design a significant effect was observed for Task ($F(3,21) = 9.674$, $p < 0.0005$, power = 0.98) but not for hand ($F(1,7) = 0.007$, $p = 0.9357$, power = 0.05). Post hoc comparisons indicated a significant difference between Fmθ changes observed during VM and those of each of the other three tasks (VM vs V: $p = 0.0005$, VM vs M: $p = 0.0015$, VM vs V + M: $p = 0.004$).

As shown in Fig. 7: right plot and in Table 2B, when cerebellar participants (n = 8) performed the VM task with the more affected hand (circles), Fmθ did not exhibit any increase. Instead, a slight decrease was observed during VM with respect to rest (-16.3 ± 17.9, SD, %, n = 8), although this change did not reach statistical significance following the Bonferroni's correction.

No significant changes in Fmθ were observed when participants performed the VM task with the less affected hand (-3.6 ± 21.4, SD, %, n = 7, see Fig. 7: right plot, squares and Table 2B).

Regarding the remaining tasks, Fig. 7: right plot and Table 2B show that Fmθ changes were negative and in general minor, reaching the level of statistical significance with respect to rest only in the V task, in the session involving the more affected hand.

When a 4 Task x 2 Hand repeated measures ANOVA was applied to the changes in Fmθ observed in cerebellar participants, no significant Task ($F(3,18) = 1.1973$, $p = 0.3390$, power = 0.08) or Hand ($F(1,6) = 0.215$, $p = 0.6592$, power = 0.05) effect could be observed.

Fig. 8 illustrates that changes in Fmθ values during VM did not exhibit any relation with participants' age, neither among control ($R = 0.155$, $p = 0.526$) nor among cerebellar participants ($R = 0.110$, $p = 0.698$). Additionally, it is noteworthy that the Fmθ ranges of the two groups showed almost no overlap.

The changes in Fmθ observed during the VM task in controls and cerebellar participants were compared by univariate ANOVA. In this analysis the age was included in the model as a covariate.

When the VM task was performed with the more affected hand (n = 8) by cerebellar participants the change in Fmθ observed was significantly lower with respect to those observed for the dominant (group effect: $F(1,16) = 21.626$, $p < 0.0005$, power = 0.99) and non-dominant (group effect: $F(1,13) = 16.385$, $p = 0.001$, power = 0.96) hands of controls (n = 11 and 8 respectively).

Similar results were obtained when the less affected hand (n = 7) of cerebellar participants was compared to the dominant (group effect: $F(1,15) = 11.852$, $p = 0.004$, power = 0.90) and non-dominant hand (group effect: $F(1,12) = 8.876$, $p = 0.012$, power = 0.78) of controls (n = 11 and 8 respectively).

Table 2
Task-related changes in Fmθ. Average ± SD values of the changes (task versus rest) in Fmθ elicited by the different tasks in the dominant (n = 11) and non-dominant (n = 8) hand of control participants and in the more (n = 8) and less affected hand (n = 7) of cerebellar participants have been displayed together with the t values, p and power levels (in bold) resulting from the statistical comparison (paired *t*-test). P values have been adjusted according to the Bonferroni's correction for multiple comparisons.

		A. Control Participants				B. Cerebellar Participants			
	Hand session	% change in θ rhythm with respect to rest	Task vs rest		Hand session	% change in θ rhythm with respect to rest	Task vs rest		
			t value	p level, ***Power***			t value	p level, ***Power***
Task								
VM	dominant	+ 29.0 ± 19.9	6.30	p < 0.0005 ***0.99***	more affected	−16.3 ± 17.9	−2.59	NS ***0.75***
	non-dominant	+ 23.1 ± 12.9	5.40	P = 0.004 ***0.99***	less affected	−3.6 ± 21.4	−0.78	NS ***0.11***
M	dominant	+ 2.5 ± 25.0	0.03	NS ***0.08***	more affected	−10.5 ± 14.8	−1.97	NS ***0.57***
	non-dominant	+ 2.0 ± 19.2	0.04	NS ***0.08***	less affected	−9.2 ± 15.0	−1.82	NS ***0.42***
V + M	dominant	+ 0.3 ± 30.6	0.45	NS ***0.05***	more affected	−8.5 ± 13.1	−1.76	NS ***0.50***
	non-dominant	+ 2.4 ± 17.5	0.12	NS ***0.10***	less affected	−13.7 ± 15.4	−2.56	NS ***0.67***
V	dominant	−5.0 ± 19.0	−1.07	NS ***0.20***	more affected	−22.4 ± 6.1	−8.51	p < 0.0005 ***1.00***
	non-dominant	+ 1.6 ± 21.6	0.16	NS ***0.07***	less affected	−11.3 ± 24.4	−1.68	NS ***0.2***

No significant age effect could be found ($p \geq 0.465$ in all instances).

3.4. Fmθ scaled with the size of the error during visuomotor task in control, but not in cerebellar participants

Since Frontal midline θ reflects error processing in the medial prefrontal cortex (Arrighi et al., 2016) and VM tracking task requires participants to monitor their performance, we tested the hypothesis that the observed increase in θ during VM in the present study correlates with the processing of an error signal. The amount of data collected allowed to reliably conduct this analysis only for the dominant hand (n = 11).

For the entire population of 11 control participants who performed the VM task with the dominant hand, the mean error rates corresponded to 0.107 ± 0.035, SD for the low error quantile, 0.289 ± 0.050, SD for the medium and 0.869 ± 0.227, SD for the high error quantile.

The increase in VM-related θ power of IC1 evaluated across the three error-based quantiles demonstrated a scaling with the magnitude of the associated errors (Fig. 9, black dots). As shown in Table 3 and Fig. 9, the highest error quantile showed the most prominent power increase, significant with respect to rest. The medium error quantile showed a medium yet significant Fmθ increase; finally the lowest error quantile displayed the smallest and non-significant increase. A 3 Error Level (low, medium, high) repeated measures ANOVA showed a significant Error level effect for the increase in Fmθ ($F(2,20) = 22.856$, $p < 0.0005$, power = 0.99). Post hoc comparisons revealed significant differences in Fmθ power changes (Table 3) between high error and low error ($p = 0.001$), as well as between medium and low error ($p = 0.002$).

We then tested whether the relation between Fmθ and performance was preserved in cerebellar participants. This analysis was conducted on the more affected hand of 5 participants from which a sufficient amount of data was collected that ensured the reliability of the analysis.

Among these cerebellar participants the mean error rates were (0.187 ± 0.089, SD,%, n = 5) for the low error quantile, (0.510 ± 0.114, SD, %, n = 5) for the medium error quantile and (1.686 ± 0.732, SD,%, n = 5) for the high error quantile.

As shown in Fig. 9 (circles) and Table 3, Fmθ failed to increase at all the three error levels. A 3 Error Level repeated measures ANOVA did not reveal any significant effect ($F(2,8) = 0.386$, $p = 0.692$, power = 0.09), indicating lack of significant differences in the Fmθ changes associated with the epochs of low, intermediate and high error level (Table 3).

A 3 Error Level repeated measures ANOVA with Group as a between-subject factor was conducted to compare the changes in Fmθ during the visuomotor (VM) task between control (n = 11) and cerebellar (n = 5) participants across the three error quantiles. This analysis revealed significant effects for Error Level ($F(2,28) = 8.092$, $p = 0.002$, power = 0.912) and Group ($F(1,14) = 14.394$, $p = 0.002$, power = 0.938) effects, while the Error Level x Group interaction was not significant ($F(2,28) = 2.496$, $p = 0.101$, power = 0.459). The low error quantile showed significantly smaller Fmθ values compared to both the medium ($p = 0.049$) and the high ($p = 0.001$) error quantiles. The significant difference in Fmθ change between controls and cerebellar participants could be confirmed for all the error classes (low: $p = 0.044$, medium: $p = 0.001$, high: $p = 0.001$).

To compare the dependance of Fmθ changes with respect to error quantiles (Fig. 9) among cerebellar (n = 5) and control (n = 11) participants, the average slope of this relationship ($(Fm\theta change_{high}\text{-}Fm\theta change_{low})/(error_{high}\text{-}error_{low})$), which represent the change in Fmθ per unit error, was computed for each subject. In control participants this value was 45.42 ± 31.25 whereas in cerebellar participants it was 5.64 ± 8.14. The difference was found to be statistically significant as indicated by a univariate ANOVA (Group effect: ($F(1, 14) = 9.388$, $p = 0.008$, power = 0.813).

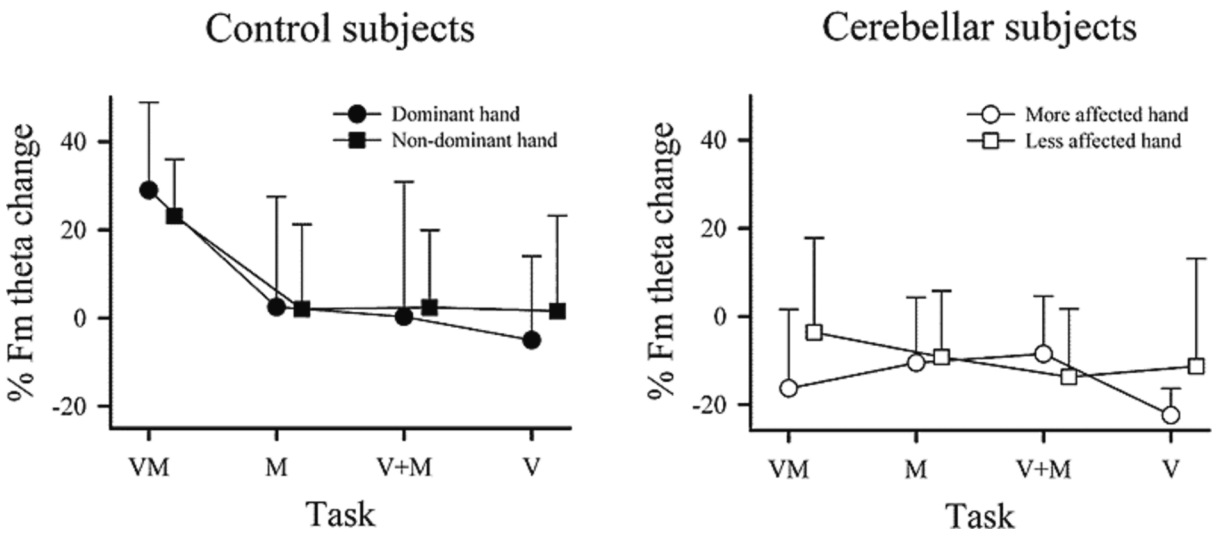

Fig. 7. *Changes in Fmθ power during the different tasks.* Left plot: Control participants. Dots and black squares represent data relative to the dominant (n = 11) and the non-dominant hand (n = 8), respectively. Right plot: Cerebellar participants. Circles and open squares represent data relative to the more affected (n = 8) and the less affected hand (n = 5), respectively. Error bars represent SD values of the mean. VM: visuomotor task. M: motor task. V + M: visual + motor task. V: visual task.

4. Discussion

4.1. General considerations

Theta activity recorded over the frontal midline cortex (Fmθ) can be considered an index of the underlying structures activation (Ishii et al., 1999; Pizzagalli et al., 2003; Tsujimoto et al., 2006). This research has explored the behaviour of Fmθ activity during a series of actions that posit a different burden on the attentional mechanisms involved in monitoring the performance of the subject. Results showed that Fmθ increased when control participants tracked a sinusoidally moving target (VM). Fmθ showed negligible changes when the participants produced a motor output without feedback of performance in the presence (V + M) or in the absence (M) of a visual distractor, or when they were engaged in a purely visual task (V). Since the tracking task imposes a strict control of motor execution, these observations suggest that Fmθ is involved in monitoring action performance.

Moreover, recruitment of the frontal midline cortices was observed during VM only when performance was moderately or highly degraded suggesting that in these conditions executive processes takes over automatic control. The increase in Fmθ during the tracking task was completely abolished in a group of participants in which cerebellum was chronically injured, indicating the essential role of this structure in the control/activation of the executive frontal midline network.

4.2. Reliability of Fmθ source separation

To isolate θ activity originating from frontal medial cortices we extracted independent components (IC) from EEG brain signals. Independent component analysis (ICA) separate individual brain signals/sources mixed by volume conduction in electroencephalographic (EEG) recordings (Delorme et al., 2012). The obtained IC estimates were robust since replication of the algorithm through ICASSO returned tight clusters of components (Himberg and Hyvarinen, 2003, 2004).

In all participants we were able to retrieve a component whose

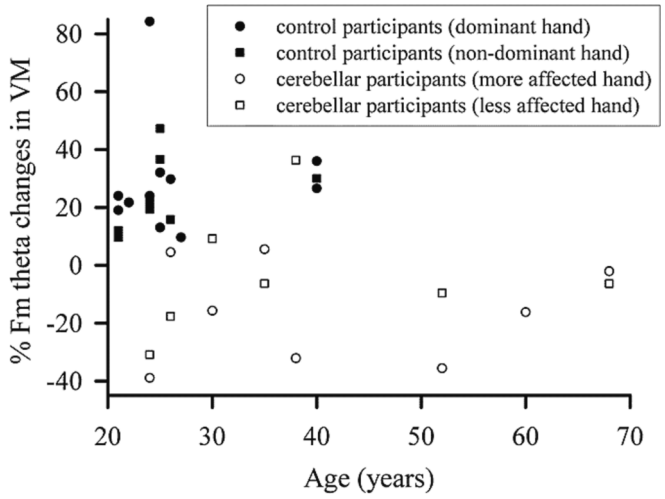

Fig. 8. *Relation between Fmθ power changes during VM and age.* Scatterplot showing the relationship between the individual % changes in Fmθ during VM task and the participant's age in control (black symbols) and cerebellar participants (white symbols). Dominant (n = 11)/non-dominant (n = 8) hand of control and more affected (n = 8)/less affected (n = 7) hand of cerebellar participants are represented as indicated in the figure inset.

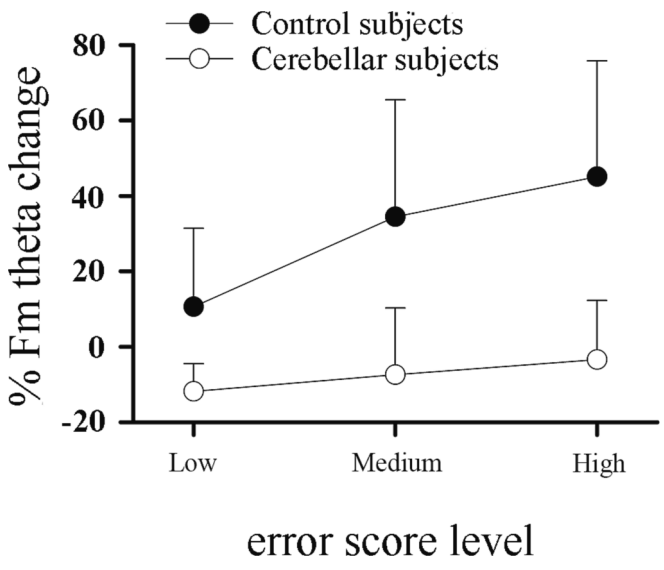

Fig. 9. *Relation between changes in Fmθ power and error score level during the VM task.* Black dots: control participants, dominant hand (n = 11). Circles: cerebellar participants, more affected hand (n = 5). Error bars represent SD values.

Table 3
Dependence of Fmθ changes upon the magnitude of the tracking errors. Values of the Fmθ changes during the VM task (task versus rest) have been separately given for the low, medium and high error score quantiles of the dominant hand of control participants and the more affected hand of cerebellar participants. The significance of the Fmθ changes (task versus rest, paired *t*-test) and the related power (in bold) have been reported below the corresponding average ± SD values for each of the three quantiles. Fmθ changes have been compared across quantiles and the relative p values of post-hoc tests are reported in the corresponding columns (Low vs Medium, High vs medium, High vs Low). P values have been adjusted according to the Bonferroni's correction for multiple comparisons.

		Error-based quantiles	Low error		Medium error		High error	
		Comparisons		Low vs Medium		High vs Medium		High vs Low
Control participants, dominant hand	n = 11	Average change in Fmθ	+10.6 ± 20.8 NS, **0.47**	P = 0.002	+34.5 ± 31.0 p < 0.002, **0.96**	NS	+45.1 ± 30.7 p < 0.0002, **0.99**	P = 0.001
		Average error score	0.107 ± 0.035		0.289 ± 0.050		0.869 ± 0.227	
Cerebellar participants, more affected hand	n = 5	Average change in θ power	−11.8 ± 7.30 NS, **0.9**	NS	−7.4 ± 17.7 NS, **0.20**	NS	−3.4 ± 15.7 NS, **0.11**	NS
		Average error score	0.187 ± 0.089		0.510 ± 0.114		1.686 ± 0.732	

activity has a spectral content in the frequency range of the θ band and whose scalp map projected over the fronto-medial region. Dipole location fitted within Brodmann areas 32 and 24, i.e. within the anterior cingulate cortex, and reproduced the ICA scalp topography with a residual variance less than 20 %.

4.3. Tracking task, forward models and prediction errors

As stated by Mattews and coll. "Tracking a moving target with the hand is a neat task to investigate the online control of visually guided movements because it relies heavily on the ability of the participant to update his/her hand motor commands on the basis of ongoing visual information" (Mattews et al., 2020). Mapping target trajectories with an optimal motor response implies a series of decision-making processes in order to dynamically adapt motor output by determining which movement or sub-movement to make and when to make it (Yoo et al., 2020). One problem arising during tracking is that afferent sensory signals have temporal delays in reaching the nervous system and movements controlled by delayed feedback show instability (Wolpert and Miall, 1996).

To cope with the delay in sensory feedback and to stabilize motor control a forward model is needed during tracking. This model predicts the future incoming sensory inflow based on a current estimate of the body state and an efferent motor control signal (Wolpert et al., 1998; McNamee and Wolpert, 2019). Predicted and actual incoming sensory signals can be combined, generating a prediction error indicating that the motor command has not produced the expected outcome. Forward models can also improve tracking effectiveness by predicting the future position of the target allowing the subject to point toward this position (Wolpert et al., 1998; McNamee and Wolpert, 2019).

4.4. Selective increase of Fmθ during the tracking task

The medial prefrontal cortices (mPFC), which include the anterior cingulate cortex (ACC), are key nodes within the network controlling executive functions. Furthermore, Fmθ reflects information processing within these regions. ACC activation and the associated Fmθ generation (Ishii et al., 1999; Pizzagalli et al., 2003; Tsujimoto et al., 2006) occur whenever an action monitoring event is required (Dehaene et al., 1998; Botvinick et al., 2001, 2004; Ridderinkhof et al., 2004), in particular during the processing of conflicting information in sensory streams (Botvinick et al., 2001, 2004; Cohen et al., 2008) and in the context of error detection (Cavanagh et al., 2009).

Given these reasons, the observation of a selective increase in Fmθ during the VM task was not unexpected.

While an increase in Fmθ may occur following both correct and incorrect responses in highly demanding tasks, Fmθ increase is a far more robust phenomenon during performance errors (Luu and Tucker, 2001; Luu et al., 2004; Yordanova et al., 2004; Trujillo and Allen. 2007). This activation serve to optimize goal-driven performance by favouring gathering of information related to contextual cues or ongoing behaviours, ultimately leading to appropriate action selection or inhibition (Dehaene et al., 1998; Botvinick et al., 2001, 2004). In the current experiments, the minimal changes in Fmθ in the V, M and V + M tasks could be attributed to the low demand that these tasks impose on participants since these task do not require the simultaneous control of sensory feedback and motor performance.

Indeed, during these tasks the subjects are not compelled to continuously monitor their performance by comparing actual to their expected outcomes, as indicated by the lack of correlated activity between visual and motor areas of the brain (Classen et al., 1998).

4.5. Fmθ during visuomotor tracking was sensitive to error and scaled with the degree of motor error

We investigated whether Fmθ oscillations during the visuomotor tracking task were significantly influenced by the magnitude of the motor error, as we have previously demonstrated in another visuomotor task (Arrighi et al., 2016). We found that the Fmθ increase scaled progressively with the extent of motor error, reaching statistical significance only during periods associated with medium and high tracking errors. These data suggest that Fmθ increases in relation to the degree of motor error once an error threshold is crossed.

The present result are in line with previous electrophysiological and brain-imaging studies that have shown that the Fmθ and the related cortical area are sensitive to error elaboration (Luu and Tucker, 2001; Luu et al., 2004; Yordanova et al., 2004; Trujillo and Allen, 2007; Anguera et al., 2009; Vocat et al., 2011; Torrecillos et al., 2014; Arrighi et al., 2016).

In the present study, the continuous nature of the task, precluded us from precisely examining the temporal dynamics of these θ changes in relation to the appearance of visual feedback or the beginning of the movement. However, a previous study designed to address this issue (Arrighi et al., 2016) reported an increase in Fmθ approximately 200 msec after the appearance of the visual feedback. It was speculated that recruitment of medial frontal cortices was triggered by a mismatch between the predicted and the actual (visually estimated) position of the arm, i.e. by a visuomotor prediction error. Savoie et al. (Savoie et al. 2018) confirmed this hypothesis demonstrating that rostral brain areas, possibly the anterior cingulate cortex, are highly sensitive to the prediction error. This hypothesis finds further support in the single unit study conducted by Yoo et al. (Yoo et al. 2020), which provides evidence that neurons in the anterior cingulate cortex can explicitly represent the predicted future position of a visually tracked target.

It is therefore reasonable to speculate that the increase in Fmθ observed during the tracking task represents the processing of a prediction error since the tracking task forces the subject to continually monitor his performance by comparing the anticipated outcomes of his action with the actual results.

4.6. Dependence of Fmθ appearance on a threshold

In both the current study and a previous one (Arrighi et al., 2016), a significant increase in Fmθ emerged after a certain threshold of error was crossed. However, the behaviour of this θ rhythm does not merely adhere to an all-or-nothing pattern. In fact, as the error magnitude grew above a certain level, θ activity exhibited a progressive increase with the growing error, suggesting a fine relationship between the development of Fmθ and the magnitude of error (Arrighi et al., 2016).

We may advance the hypothesis that the executive network is activated only when this error surpasses a certain threshold at which point it becomes sensitive to the magnitude of error. According to this model the executive network is recruited by the prediction error when mismatch between action and sensory consequences exceeds a specific threshold. This occurs when the compensation by implicit automatic mechanisms becomes impossible. In such cases, awareness of a conflict emerges and a frontal executive network needs to be further recruited for successfully carrying out the task (Andre and Arrighi, 2003; Arrighi et al., 2016).

4.7. Lack of Fmθ increase during the tracking task in cerebellar participants

Unlike the control participants, those bearing a chronic damage of the cerebellum did not exhibit an increase in Fmθ when performing the tracking task. Actually, a slight decrease was observed during VM in cerebellar participants performing the task with their more affected hand, which did not reach the level of statistical significance. The reliability of this decrease has to be further investigated in a larger sample of subjects, so to enhance the power of the observation. In any case the difference in Fmθ changes during VM task observed between control and cerebellar participants was significant and robust (power = 0.99).

The relation between Fmθ and degree of tracking error was also severely blunted in cerebellar participants. Cerebellar participants did not show an increase of Fmθ during the task, but rather a slight decrease which was not significantly modified by the error level, not even during the epochs associated with the highest error quantile. This lack of scaling occurred despite the cerebellar participants performed significantly worse than control participants.

In the present study, the ages of control and cerebellar participants were different: this represent a limitation of the study. However, as shown in Fig. 8, the changes in Fmθ observed during VM task were independent upon age and their values showed almost no overlap in the two groups. Finally, the difference in Fmθ between control and cerebellar participants was significant also when the age was inserted as a covariate in the ANOVA model.

If we consider the expression of Fmθ in the frontal midline cortices as an hallmark of prediction error we can interpret the absence of an Fmθ increase during error occurrence in cerebellar participants as being due to the inability of the damaged cerebellar structures to generate and transmit this signal to the cortical network.

First of all, the cerebellum is considered essential for correcting errors resulting from inaccuracies in behaviour (Takagi et al., 1998; Lee et al., 2012).

It is believed that the cerebellum achieves error correction by generating predictions of the sensory consequences of a command which are then compared with the actual outcome to generate a prediction error. This process relies on the use of an internal model.

A substantial body of evidence from clinical studies, human neuroimaging and non-invasive stimulation studies supports the hypothesis that internal-forward-models are stored within the cerebellum (Wolpert and Miall, 1996; Wolpert et al., 1998; Imamizu et al., 2000; Ebner and Pasalar, 2008; Kakei et al., 2019; Popa and Ebner, 2019; McNamee and Wolpert, 2019). These data are consistent with the results of experiments showing that individual cerebellar neurons (mossy fibers, Purkinje cells and nuclear neurons) may code both current and future states of the body (Roitman et al., 2005; Pasalar et al., 2006; Ebner and Pasalar, 2008; Popa and Ebner, 2019; Tanaka et al., 2019, 2020; see however Yamamoto et al., 2007).

There is evidence that the tracking task we employed activates the cerebellum which is crucial for its successful execution. In healthy subjects, functional imaging has shown changes in cerebellar activation following tracking movement (Imamizu et al., 2000). Additionally lesion of white matter of the right cerebellar hemisphere around dentate nucleus and bilaterally in the cerebellar peduncles had been shown to impair “on-line” visuomotor control in a wrist and arm tracking task (Liu et al., 1999).

The tracking task requires a predictive forward model to be performed correctly (Miall and Reckess, 2002). The impairment of performance and the lack of an increase in Fmθ we observed in cerebellar participants is consistent with the absence of a predictive signal. Savoie et al. (Savoie et al. 2018) documented that the mid frontal cortices express θ activity when prediction errors occur.

Multiple communication pathways between the cerebellum and neocortical structures are present. These pathways may allow the predictive signal generated within the cerebellum to influence the cortical network responsible for the tracking movement. This nework includes sensory, motor, association and executive cortices (Classen et al., 1998).

It is believed that cerebrocerebellar communication is based on loops where cortical projection zones to the cerebellum are also recipient structures from the cerebellum (Andre and Arrighi, 2003; Ramnani, 2006). In humans, it has been shown that several networks related to specific functions are mapped onto cerebellar regions (Kipping et al., 2013; Kipping et al., 2017) and all of them involve the medial prefrontal/cingulate cortex (Kipping et al., 2013).

In addition to a “direct” cerebello-frontal pathway, predictions error may recruit the prefrontal cortex through cortico-cortical connections, such as those running through the medial parietal cortex. Within this region, the precuneus is involved in processing spatially guided behaviour, in elaborating the body scheme and can be associated with conscious aspects of error processing. It may become activated when the discrepancy between predicted and actual sensory consequence of movement modulates the sense of agency (Cavanna and Trimble, 2006; Cavanna, 2007).

In the present study, the lesions in the cerebellar participants affected the hemivermis of the posterior lobe and the respective cerebellar hemisphere. Therefore as a limitation of this study, we are unable to differentiate the specific output channel(s) involved in transmitting to the cortex the prediction error.

Finally, there is evidence that the θ activity generated within the cortical network can flow to the cerebellum and vice versa. As proposed by Andre and Arrighi (Andre and Arrighi, 2003), cerebello-cortical communication requires that the neurons within these two structures become entangled through neuronal oscillations using specific frequency bands. Various distinct cortical rhythms (reviewed in Andre and Arrighi, 2003) are expressed in both the cortex and the cerebellum including the θ rhythm. The cerebellum exhibits θ-band activity correlated with that of the premotor and motor areas during bimanual voluntary tasks in humans (Gross et al., 2005; Schnitzler et al., 2006).

In humans, cerebellar TMS studies have shown that the cerebellum can evoke θ activity within the frontal cortex (Schutter and van Honk, 2006; Singh et al., 2019). In this context, reciprocally, Ros et al. reported that “neocortical output entrains and drives cerebellar network activity and generates a cerebellar LFP and electroencephalogram (EEG) that is similar to that of the neocortex, which results in part through the activation of granule, Golgi, and Purkinje neurons” (Ros et al., 2009).

We propose that the θ rhythm may serve as a means of

communicating the prediction error generated in the cerebellum to the cortex. Prediction error arises because a copy of the neural cortical motor command reaches the cerebellum, where it is transformed into a pattern of activity representing the expected sensory outcome (see Wolpert and Miall, 1996). Within the cerebellum, this pattern is then compared to the actual incoming sensory information and a mismatch may occur. We suggest that, when such a mismatch occurs, the θ rhythm is amplified within the cerebellum and entrains the cerebral cortical target within the same frequency range.

It is of interest that in both the present and our previous study (Arrighi et al., 2016) Fmθ began to increase only after crossing an error threshold. Previous research has shown that the cerebellum possesses two types of output channels (Steriade, 2003): one type impinges upon the specific thalamic nuclei which have a focused projection to the cortex, while the other impinges onto the a-specific nuclei such as the intralaminar nuclei with a more diffuse influence on the cortex including the prefrontal cortex. The two systems are not entirely segregated, as the specific system may send sparse collaterals to the a-specific system.

It has been proposed (Andre and Arrighi, 2003) that when the predicted error signals are low, their neural representations are funnelled to the cortex via the specific system. This process modifies the cortical activity pattern within areas involved in implicit perceptual motor processes such as the posterior parietal lobe and the premotor/motor cortex.

In contrast, when the mismatch between anticipation and the outcome is large (crossing the threshold for automatic correction), the error signal is also large and its representation spreads to the a-specific system with enough strength to activate it. The ignition of the a-specific system allows for a spatial spread of oscillatory θ patterns to the frontal cortex, activating executive processes that coordinates a broad cortical network to elicit conscious monitoring and voluntary strategies for error correction (Friedman and Robbins, 2022).

4.8. Conclusions

In conclusion, our data indicate that the cerebellum is necessary for supplying the medial prefrontal cortex (mPFC) with prediction error-related information. It is likely that this information is generated within the cerebellum as a theta oscillation and entrains the frontal cortical network. This occurs when automatic control falters, and a deliberate correction mechanism needs to be triggered. Further studies are needed to verify if this alerting function also occurs in the context of the other cognitive and non-cognitive functions in which the cerebellum is involved (Schmahmann, 1996, 2019; Strick et al., 2009).

Funding

This research did not receive any specific grant from funding agencies in the public, commercial, or not-for-profit sectors.

CRediT authorship contribution statement

P. Andre: Conceptualization, Formal analysis, Investigation, Methodology, Project administration, Software, Writing – original draft, Writing – review & editing. **N. Cantore:** Investigation, Data curation. **L. Lucibello:** Visualization, Writing – review & editing. **P. Migliaccio:** Visualization, Data curation. **B. Rossi:** Resources, Supervision. **M.C. Carboncini:** Resources, Supervision. **A.M. Aloisi:** Resources, Supervision. **D. Manzoni:** Formal analysis, Writing – review & editing. **P. Arrighi:** Data curation, Methodology, Formal analysis, Software, Writing – original draft.

Declaration of competing interest

The authors declare that they have no known competing financial interests or personal relationships that could have appeared to influence the work reported in this paper.

Data availability

Data will be made available on request.

References

Andre, P., Arrighi, P., 2003. Hipnic modulation of cerebellar information processing: implications for the cerebro-cerebellar dialogue. Cerebellum 2, 84–95. https://doi.org/10.1080/14734220309403.

Anguera, J.A., Seidler, R.D., Gehring, W.J., 2009. Changes in performance monitoring during sensorimotor adaptation. J. Neurophsyol. 102, 1868–1879. https://doi.org/10.1152/jn.00063.2009.

Arrighi, P., Bonfiglio, L., Minichilli, F., Cantore, N., Carboncini, M.C., Piccotti, E., Rossi, B., Andre, P., 2016. EEG theta dynamics within frontal and parietal cortices for error processing during reaching movements in a prism adaptation study altering visuo-motor predictive planning. PLoS One 11 (3), e0150265.

Botvinick, M.M., Braver, T.S., Barch, D.M., Carter, C.S., Cohen, J.D., 2001. Conflict monitoring and cognitive control. Psychol. Rev. 108, 624–652. https://doi.org/10.1037/0033-295x.108.3.624.

Botvinick, M.M., Cohen, J.D., Carter, C.S., 2004. Conflict monitoring and anterior cingulate cortex: an update. Trends Cogn. Sci. 8, 539–546. https://doi.org/10.1016/j.tics.2004.10.003.

Botvinick MM. Conflict monitoring and decision making: Reconciling two perspectives on anterior cingulate function. Cogn. Affect. Behav. Neurosci. 2007; 7: 356-66. https://doi.org/ 10.3758/cabn.7.4.356.

Brodal, P., 1978. The corticopontine projection in the rhesus monkey. Origin and principles of organization. Brain 101, 251–283. https://doi.org/10.1093/brain/101.2.251.

Carter CS, Braver TS, Barch DM, Botvinick MM, Noll D, Cohen JD. Anterior cingulate cortex, error detection, and the online monitoring of performance. Science 1998; 280: 747-9. https://doi.org/ 10.1126/science.280.5364.747.

Cavanagh, J.F., Cohen, M.X., Allen, J.J.B., 2009. Prelude to and resolution of an error: EEG phase synchrony reveals cognitive control dynamics during action monitoring. J. Neurosci. 29, 98–105. https://doi.org/10.1523/JNEUROSCI.4137-08.2009.

Cavanna, A.E., 2007. The precuneus and consciousness. CNS Spectr. 12, 545–552. https://doi.org/10.1017/s1092852900021295.

Cavanna, A.E., Trimble, M.R., 2006. The precuneus: a review of its functional anatomy and behavioural correlates. Brain 129, 564–583. https://doi.org/10.1093/brain/awl004.

Classen, J., Gerloff, C., Honda, M., Hallett, M., 1998. Integrative visuomotor behavior is associated with interregionally coherent oscillations in the human brain. J. Neurophysiol. 79, 1567–1573. https://doi.org/10.1152/jn.1998.79.3.1567.

Cohen, M.X., Ridderinkhof, K.R., Haupt, S., Elger, C.E., Fell, J., 2008. Medial frontal cortex and response conflict: evidence from human intracranial EEG and medial frontal cortex lesion. Brain Res. 1238, 127–142. https://doi.org/10.1016/j.brainres.2008.07.114.

Contreras-Vidal, J.L., Kerick, S.E., 2004. Independent component analysis of dynamic brain responses during visuomotor adaptation. Neuroimage 21, 936–945. https://doi.org/10.1016/j.neuroimage.2003.10.037.

Corbetta, M., Miezin, F.M., Dobmeyer, S., Shulman, G.L., Petersen, S.E., 1991. Selective and divided attention during visual discriminations of shape, color, and speed: functional anatomy by positron emission tomography. J. Neurosci. 11, 2383–2402. https://doi.org/10.1523/JNEUROSCI.11-08-02383.1991.

Dehaene, S., Kerszberg, M., Changeux, J.P., 1998. A neuronal model of a global workspace in effortful cognitive tasks. Proc. Natl. Acad. Sci. USA 95, 14529–14534. https://doi.org/10.1073/pnas.95.24.14529.

Delorme, A., Palmer, J., Onton, J., Oostenveld, R., Makeig, S., 2012. Independent EEG sources are dipolar. PLoS One 7 (2), e30135.

Desmurget, M., Grafton, S., 2000. Forward modeling allows feedback control for fast reaching movements. Trends Cogn. Sci. 4, 423–431. https://doi.org/10.1016/s1364-6613(00)01537-0.

Diedrichsen, J., Hashambhoy, Y., Rane, T., Shadmehr, R., 2005. Neural correlates of reach errors. J. Neurosci. 25, 9919–9931. https://doi.org/10.1523/JNEUROSCI.1874-05.2005.

Diedrichsen, J., Criscimagna-Hemminger, S.E., Shadmehr, R., 2007. Dissociating timing and coordination as functions of the cerebellum. J. Neurosci. 27, 6291–6301. https://doi.org/10.1523/JNEUROSCI.0061-07.2007.

Dum, R.P., Strick, P.L., 2003. An Unfolded Map of the Cerebellar Dentate Nucleus and its Projections to the Cerebral Cortex. J. Neurophysiol. 89, 634–669. https://doi.org/10.1152/jn.00626.2002.

Ebner, T.J., Pasalar, S., 2008. Cerebellum Predicts the Future Motor State. Cerebellum 7, 583–588. https://doi.org/10.1007/s12311-008-0059-3.

Falkenstein, M., Hohnsbein, J., Hoormann, J., Blanke, L., 1991. Effects of crossmodal divided attention on late ERP components. II. Error processing in choice reaction tasks. Electroencephalogr. Clin. Neurophysiol. 78 (447–55) https://doi.org/10.1016/0013-4694(91)90062-9.

Flament, D., Ellermann, J.M., Kim, S.G., Ugurbil, K., Ebner, T.J., 1996. Functional magnetic resonance imaging of cerebellar activation during the learning of a visuomotor dissociation task. Hum. Brain Map. 4, 210–226. https://doi.org/10.1002/hbm.460040302.

Friedman, N.P., Robbins, T.W., 2022. The role of prefrontal cortex in cognitive control and executive function. Neuropsychopharmacology 47, 72–89. https://doi.org/10.1038/s41386-021-01132-0.
Gatti, D., Rinaldi, L., Ferreri, L., Vecchi, T., 2021. The Human Cerebellum as a Hub of the Predictive Brain. Brain Sci. 11 (11), 1492. https://doi.org/10.3390/brainsci11111492.
Giannetti, S., Molinari, M., 2002. Cerebellar input to the posterior parietal cortex in the rat. Brain Res. Bull. 58, 481–489. https://doi.org/10.1016/S0361-9230(02)00815-8.
Glickstein, M., May 3rd, J.G., Mercier, B.E., 1985. Corticopontine projection in the macaque: the distribution of labelled cortical cells after large injections of horseradish peroxidase in the pontine nuclei. J. Comp. Neurol. 235, 343–359. https://doi.org/10.1002/cne.902350306.
Grafton ST, Schmitt P, Van H J, Diedrichsen J. Neural substrates of visuomotor learning based on improved feedback control and prediction. Neuroimage 2008; 39: 1383–95. https://doi.org/ 10.1016/j.neuroimage.2007.09.062.
Gross J, Pollok B, Dirks M, Timmermann L, Butz M, and Schnitzler A. Task-dependent oscillations during unimanual and bimanual movements in the human primary motor cortex and SMA studied with magnetoencephalography. Neuroimage 2005; 26: 91–98. https://doi.org/ 10.1016/j.neuroimage.2005.01.025.
Habas, C., 2021. Functional Connectivity of the Cognitive Cerebellum. Front. Syst. Neurosci. 15, 642225 https://doi.org/10.3389/fnsys.2021.642225.
Himberg, J., Hyvärinen, A., Esposito, F., 2004. Validating the independent components of neuroimaging time series via clustering and visualization. Neuroimage 22, 1214–1222. https://doi.org/10.1016/j.neuroimage.2004.03.027.
Himberg J. and Hyvarinen A."Icasso: software for investigating the reliability of ICA estimates by clustering and visualization, "2003 IEEE XIII Workshop on Neural Networks for Signal Processing", (IEEE Cat. No.03TH8718), 2003, pp. 259-68. https://doi.org/10.1109/NNSP.2003.1318025.
Hyvärinen, A, Oja, E., 2000. Independent component analysis: algorithms and applications. Neural Netw. 13, 411–430. https://doi.org/10.1016/s0893-6080(00)00026-5.
Imamizu, H., Miyauchi, S., Tamada, T., Sasaki, Y., Takino, R., Putz, B., Yoshioka, T., Kawato, M., 2000. Human cerebellar activity reflecting an acquired internal model of a new tool. Nature 403, 192–195. https://doi.org/10.1038/35003194.
Ishii, R., Shinosaki, K., Ukai, S., Inouye, T., Ishihara, T., Yoshimine, T., Hirabuki, N., Asada, H., Kihara, T., Robinson, S.E., Takeda, M., 1999. Medial prefrontal cortex generates Fmθ rhythm. Neuroreport 10, 675–679. https://doi.org/10.1097/00001756-199903170-00003.
Ito, M., 2005. Bases and implications of learning in the cerebellum – adaptive control and internal model mechanism. Prog. Brain Res. 148, 95–109. https://doi.org/10.1016/S0079-6123(04)48009-1.
Kakei, S., Lee, J., Mitoma, H., Tanaka, H., Manto, M., Hampe, C.S., 2019. Contribution of the Cerebellum to Predictive Motor Control and Its Evaluation in Ataxic Patients. Front. Hum. Neurosci. 13, 216. https://doi.org/10.3389/fnhum.2019.00216.
Kiehl, K.A., Liddle, F.P., Hopfinger, J.B., 2000. Error processing and the rostral anterior cingulate: an event-related fMRI study. Psychophysiology 37, 216–223.
Kipping JA, Tuan TA, Fortier MV, Qiu A. Cereb Cortex. Asynchronous Development of Cerebellar, Cerebello-Cortical, and Cortico-Cortical Functional Networks in Infancy, Childhood, and Adulthood. Cereb. Cortex 2017; 27: 5170-84. https://doi.org/10.1016/10.1093/cercor/bhw298.
Kipping, J.A., Grodd, V., Kumar, V., Taubert, M., Villringer, A., Margulies, D.S., 2013. Overlapping and parallel cerebello-cerebral networks contributing to sensorimotor control: An intrinsic functional connectivity study. Neuroimage 83, 837–848. https://doi.org/10.1016/j.neuroimage.2013.07.027.
Klimesch, W., 1999. EEG alpha and theta oscillations reflect cognitive and memory performance: a review and analysis. Brain Res. Rev. 29, 169–195. https://doi.org/10.1016/s0165-0173(98)00056-3.
Lee, J., Kagamihara, Y., Tomatsu, S., Kakei, S., 2012. The Functional Role of the Cerebellum in Visually Guided Tracking Movement. Cerebellum 11, 426–433. https://doi.org/10.1007/s12311-012-0370-x.
Liu, X., Ingram, H.A., Palace, J.A., Miall, R.C., 1999. Dissociation of 'on-line' and 'off-line' visuomotor control of the arm by focal lesions in the cerebellum and brainstem. Neurosci. Lett. 264, 121–124. https://doi.org/10.1016/S0304-3940(99)00165-2.
Luu, P., Tucker, D.M., 2001. Regulating action: alternating activation of midline frontal and motor cortical networks. Clin. Neurophysiol. 112, 1295–1306. https://doi.org/10.1016/s1388-2457(01)00559-4.
Luu, P., Tucker, D.M., Makeig, S., 2004. Frontal midline theta and the error-related negativity: neurophysiological mechanisms of action regulation. Clin. Neurophysiol. 115, 1821–1835. https://doi.org/10.1016/j.clinph.2004.03.031.
Mathew, J., Masson, G.S., Danion, F.R., 2020. Sex differences in visuomotor tracking. Sci. Rep. 10 (1), 11863. https://doi.org/10.1038/s41598-020-68069-0.
McNamee, D., Wolpert, D.M., 2019. Internal Models in Biological Control. Annu. Rev. Control Robot Auton. Syst. 2, 339–364. https://doi.org/10.1146/annurev-control-060117-105206.
Miall, R.C., Reckess, G.Z., 2002. The cerebellum and the timing of coordinated eye and hand tracking. Brain Cogn. 48, 212–226. https://doi.org/10.1006/brcg.2001.1314.
Miall, R.C., Weir, D.J., Wolpert, D.M., Stein, J.F., 1993. Is the Cerebellum a Smith Predictor? J. Mot. Behav. 25, 203–216. https://doi.org/10.1080/00222895.1993.9942050.
Miall, R.C., Christensen, L.O., Cain, O., Stanley, J., 2007. Disruption of state estimation in the human lateral cerebellum. PLoS Biol. 5, e316.
Mutha, P.K., Sainburg, R.L., Haaland, K.Y., 2011. Critical neural substrates for correcting unexpected trajectory errors and learning from them. Brain 134, 3647–3661. https://doi.org/10.1093/brain/awr275.
Neuper, C., Wörtz, M., Pfurtscheller, G., 2006. ERD/ERS patterns reflecting sensorimotor activation and deactivation. Prog. Brain Res. 159, 211–222. https://doi.org/10.1016/S0079-6123(06)59014-4.
Onton, J., Delorme, A., Makeig, S., 2005. Frontal midline EEG dynamics during working memory. Neuroimage 27, 341–356. https://doi.org/10.1016/j.neuroimage.2005.04.014.
Pasalar, S., Roitman, A.V., Durfee, W.K., Ebner, T.J., 2006. Force field effects on cerebellar Purkinje cell discharge with implications for internal models. Nat. Neurosci. 9, 1404–1411. https://doi.org/10.1038/nn1783.
Pizzagalli, D.A., Oakes, T.R., Davidson, R.J., 2003. Coupling of theta activity and glucose metabolism in the human rostral anterior cingulate cortex: an EEG/PET study of normal and depressed subjects. Psychophysiology 40, 939–949. https://doi.org/10.1111/1469-8986.00112.
Popa, L.S., Ebner, T.J., 2019. Cerebellum, Predictions and Errors. Front. Cell. Neurosci. 12, 524. https://doi.org/10.3389/fncel.2018.00524.
Popa, L.S., Hewitt, A.L., Ebner, T.J., 2013. Purkinje cell simple spike discharge encodes error signals consistent with a forward internal model. Cerebellum 12, 331–333. https://doi.org/10.1007/s12311-013-0452-4.
Ramnani, N., 2006. The primate cortico-cerebellar system: anatomy and function. Nat. Rev. Neurosci. 7, 511–522. https://doi.org/10.1038/nrn1953.
Ramnani, N., 2012. Frontal lobe and posterior parietal contributions to the cortico-cerebellar system. Cerebellum 11, 366–383. https://doi.org/10.1007/s12311-011-0272-3.
Ridderinkhof, K.R., Ullsperger, M., Crone, E.A., Nieuwenhuis, S., 2004. The role of the medial frontal cortex in cognitive control. Science 306, 443–447. https://doi.org/10.1126/science.1100301.
Roitman, A.V., Pasalar, S., Johnson, M.T., Ebner, T.J., 2005. Position, direction of movement, and speed tuning of cerebellar Purkinje cells during circular manual tracking in monkey. J. Neurosci. 25, 9244–9257. https://doi.org/10.1523/JNEUROSCI.1886-05.2005.
Ros, H., Sachdev, R.N., Yu, Y., Sestan, N., McCormick, D.A., 2009. Neocortical networks entrain neuronal circuits in cerebellar cortex. J. Neurosci. 29, 10309–11020. https://doi.org/10.1523/JNEUROSCI.1886-05.2005.
Savoie, F.A., Thénault, F., Whittingstall, K., Bernier, P.M., 2018. Visuomotor Prediction Errors Modulate EEG Activity Over Parietal Cortex. Sci. Rep. 8, 12513. https://doi.org/10.1038/s41598-018-30609-0.
Schlerf, J.E., Ivry, R.B., Diedrichsen, J., 2012. Encoding of sensory prediction errors in the human cerebellum. J. Neurosci. 32, 4913–4922. https://doi.org/10.1523/JNEUROSCI.4504-11.2012.
Schmahmann, J.D., 1996. From Movement to Thought: Anatomic Substrates of the Cerebellar Contribution to Cognitive Processing. Hum. Brain Mapp. 4, 174–198. https://doi.org/10.1002/(SICI)1097-0193(1996)4:3%3C174::AID-HBM3%3E3.0.CO;2-0.
Schmahmann, J.D., 2019. The cerebellum and cognition. Neurosci. Lett. 688, 62–75. https://doi.org/10.1016/j.neulet.2018.07.005.
Schnitzler, A., Timmermann, L., Gross, J., 2006. Physiological and pathological oscillatory networks in the human motor system. J. Physiol. Paris 99, 3–7. https://doi.org/10.1016/j.jphysparis.2005.06.010.
Schutter, D.J., van Honk, J., 2006. An electrophysiological link between the cerebellum, cognition and emotion: frontal theta EEG activity to single-pulse cerebellar TMS. Neuroimage 33, 1227–1231. https://doi.org/10.1016/j.neuroimage.2006.06.055.
Singh, A., Trapp, N.T., De Corte, B., Cao, S., Kingyon, J., Boes, A.D., Parker, K.L., 2019. Cerebellar Theta Frequency Transcranial Pulsed Stimulation Increases Frontal Theta Oscillations in Patients with Schizophrenia. Cerebellum 18, 489–499. https://doi.org/10.1007/s12311-019-01013-9.
Steriade, M., 2003. Cerebello-cerebral interactions during states of vigilance. Cerebellum 2, 82–83. https://doi.org/10.1080/14734220309404.
Streng, M.L., Popa, L.S., Ebner, T.J., 2018a. Complex spike wars: a new hope. Cerebellum 17, 735–746. https://doi.org/10.1007/s12311-018-0960-3.
Streng, M.L., Popa, L.S., Ebner, T.J., 2018b. Modulation of sensory prediction error in Purkinje cells during visual feedback manipulations. Nat. Commun. 9, 1099. https://doi.org/10.1038/s41467-018-03541-0.
Strick, P.L., Dum, R.P., Fiez, J.A., 2009. Cerebellum and nonmotor function. Annu Rev. Neurosci. 32, 413–434. https://doi.org/10.1146/annurev.neuro.31.060407.125606.
Takagi M, Zee DS, Tamargo RJ. Effects of lesions of the oculomotor vermis on eye movements in primate: saccades. J. Neurophysiol. 1998; 80:1911–31. https://doi.org/ 10.1152/jn.1998.80.4.1911.
Tanaka, H., Ishikawa, T., Kakei, S., 2019. Neural Evidence of the Cerebellum as a State Predictor. Cerebellum 18, 349–371. https://doi.org/10.1007/s12311-018-0996-4.
Tanaka, H., Ishikawa, T., Lee, J., Kakei, S., 2020. The cerebro-cerebellum as a locus of forward model: A review. Front. Syst. Neurosci. 14, 19. https://doi.org/10.3389/fnsys.2020.00019.
Torrecillos, F., Albouy, P., Brochier, T., Malfait, N., 2014. Does the processing of sensory and reward-prediction errors involve common neural resources? Evidence from a frontocentral negative potential modulated by movement execution errors. J. Neurosci. 34, 4845–4856. https://doi.org/10.1523/JNEUROSCI.4390-13.2014.
Trujillo, L.T., Allen, J.J., 2007. Theta EEG dynamics of error-related negativity. Clin. Neurophysiol. 118, 645–668. https://doi.org/10.1016/j.clinph.2006.11.009.
Tsujimoto, T., Hideki, S., Yoshikazu, I., 2006. Direct recording of theta oscillations in primate prefrontal and anterior cingulate cortices. J. Neurophysiol. 95, 2987–3000. https://doi.org/10.1152/jn.00730.2005.
Vilensky, J.A., Hoesen, G.W.V., 1981. Corticopontine projections from the cingulate cortex in the rhesus monkey. Brain Res. 205, 391–395. https://doi.org/10.1016/0006-8993(81)90348-6.

Vocat, R., Pourtois, G., Vuilleumier, P., 2011. Parametric modulation of error-related ERP components by the magnitude of visuo-motor mismatch. Neuropsychologia 49, 360–367. https://doi.org/10.1016/j.neuropsychologia.2010.12.027.
Wolpert, D.M., Ghahramani, Z., Jordan, M.I., 1995. An internal model for sensorimotor integration. Science 269, 1880–1882. https://doi.org/10.1126/science.7569931.
Wolpert, D.M., Miall, R.C., 1996. Forward models for physiological motor control. Neural Netw. 9, 1265–1279. https://doi.org/10.1016/s0893-6080(96)00035-4.
Wolpert, D.M., Miall, R.C., Kawato, M., 1998. Internal models in the cerebellum. Trends Cogn. Sci. 2, 338–347. https://doi.org/10.1016/s1364-6613(98)01221-2.
Yamamoto, K., Kawato, M., Kotosaka, S., Kitazawa, S., 2007. Encoding of movement dynamics by Purkinje cell simple spike activity during fast arm movements under resistive and assistive force fields. J. Neurophysiol. 97, 1588–1599. https://doi.org/10.1152/jn.00206.2006.
Yoo, S.B.M., Tu, J.C., Piantadosi, S.T., Hayden, B.Y., 2020. The neural basis of predictive pursuit. Nat. Neurosci. 23, 252–259. https://doi.org/10.1038/s41593-019-0561-6.
Yordanova, J., Falkenstein, M., Hohnsbein, J., Kolev, V., 2004. Parallel systems of error processing in the brain. Neuroimage 22, 590–602. https://doi.org/10.1016/j.neuroimage.2004.01.040.